

## CHEMICAL STATE OF GOLD DEPOSITED FROM QUENCHED Mg-S-H-O FLUIDS BY X-RAY PHOTOELECTRON SPECTROSCOPY

STEPHEN W. KNIPE AND MICHAEL E. FLEET<sup>1</sup>

*Department of Earth Sciences, University of Western Ontario, London, Ontario N6A 5B7*

### ABSTRACT

Reaction of MgS, H<sub>2</sub>O, and Au at 100 to 900°C and 0.15 GPa yields quenched products of brucite or periclase (or both), S-Au-bearing fluid, and H<sub>2</sub>S gas. The composition and chemical states in surface layers of dried solid and evaporated fluid products have been determined by X-ray photoelectron spectroscopy (XPS). Gold and S occur in variable proportions, but minimum S: Au ratios are ~1. A significant to dominant component in all Au 4f XPS spectra exists, with a 4f<sub>7/2</sub> peak shifted positive in binding energy relative to Au<sup>0</sup> at 84.0 eV. In solid products dried in air, this peak is at 85.3 eV (±0.2 eV), and is assigned to Au<sup>+</sup>. The accompanying S 2p spectra are composite, but have a main peak at ~162.4 eV corresponding to hydrosulfide (HS<sup>-</sup>). Re-analysis of these solid products after exposure to air and daylight for several weeks revealed Au<sup>0</sup> only, and sulfate (S 2p peak at >168.0 eV) became the dominant S species. The Au 4f XPS spectra of solids from capsules opened in an inert atmosphere and dried in vacuum and of both air- and vacuum-dried fluids are dominated by a Au species with a 4f<sub>7/2</sub> peak at 84.5 and 84.3 eV, respectively, which is attributed to either nanoscale clusters of Au atoms or mononuclear Au<sup>0</sup>. These results support the predominance of Au<sup>+</sup> in aqueous sulfidic ore fluids, may have bearing for a Au-cluster component of invisible Au in arsenian pyrite and arsenopyrite, and demonstrate the deposition of Au by loss of H<sub>2</sub>S and reduction in the absence of metal sulfides.

**Keywords:** gold, X-ray photoelectron spectroscopy (XPS), precipitation of gold, Au-S-H complexes, Mg-S-H-O-Au system.

### SOMMAIRE

La réaction de MgS, H<sub>2</sub>O, et Au entre 100 et 900°C à 0.15 GPa donne, comme produits, brucite ou périclase (ou les deux), une phase fluide contenant S et Au, et un gaz, H<sub>2</sub>S. La composition et l'état des niveaux de surface des solides séchés et de la phase fluide évaporée ont été caractérisés par spectroscopie des photoélectrons X (XPS). L'or et le soufre se présentent en proportions variables, mais le rapport minimum de S à Au est environ 1. L'or 4f est une composante importante ou même dominante de tous les spectres XPS; le pic 4f<sub>7/2</sub> est déplacé vers une valeur positive dans son énergie de liaison par rapport à Au<sup>0</sup>, à 84.0 eV. Dans les produits solides séchés à l'air, ce pic se trouve à 85.3 eV (±0.2 eV), et serait dû à Au<sup>+</sup>. Les spectres pour le soufre 2p sont composites, mais le pic principal à environ 162.4 eV correspond au bisulfure. Une nouvelle analyse des produits solides après interaction avec l'air et lumière naturelle pour plusieurs semaines révèle la présence de Au<sup>0</sup> seulement, tandis que le sulfate (pic de S 2p à >168.0 eV) est devenu l'espèce dominante du soufre. Les spectres XPS de l'or 4f dans les solides séparés des capsules ouvertes dans un atmosphère inerte et séchés sous vide et dans la phase fluide, évaporée à l'air ou sous vide, contiennent surtout une espèce aurifère ayant un pic 4f<sub>7/2</sub> à 84.5 et 84.3 eV, respectivement, que nous attribuons à des regroupements d'atomes d'or à une échelle nanométrique, ou à l'espèce mononucléaire Au<sup>0</sup>. Ces résultats concordent avec la prédominance de Au<sup>+</sup> dans une phase fluide aurifère aqueuse contenant du soufre, et pourrait bien expliquer la formation d'agglomérations d'atomes d'or, composant d'or dit invisible dans la pyrite arsénifère et l'arsénopyrite. De plus, ils démontrent la possibilité de déposer l'or par perte de H<sub>2</sub>S et réduction en l'absence de sulfures de métaux.

(Traduit par la Rédaction)

**Mots-clés:** or, spectroscopie des photoélectrons X, précipitation de l'or, complexes Au-S-H, système Mg-S-H-O-Au.

### INTRODUCTION

Aqueous hydrosulfide complexes are believed to be extremely important in the transport of Au in ore fluids (Seward 1973), particularly in the case of aqueous fluids that are S-rich, Cl-poor, reducing, and below ~350°C (Seward 1991). Compelling indirect evidence

exists for two dominant hydrosulfide species in Au transport [Au(HS)<sub>2</sub><sup>-</sup> and AuHS<sup>0</sup>; e.g., Benning & Seward 1996], but direct confirmation of Au<sup>+</sup>-S species in aqueous solution remains experimentally very difficult. Recent experiments (Fleet & Knipe, in progress) reveal high contents of dissolved Au in fluids in the system Mg-S-H-O system, due to the high partial

<sup>1</sup> To whom correspondence should be addressed. *E-mail address:* mfleet@julian.uwo.ca

pressure of  $\text{H}_2\text{S}$  generated by using  $\text{MgS}$  as a reagent in closed hydrothermal reactions. The correspondingly high contents of Au measured in quenched products of these hydrothermal Mg–S–H–O experiments made feasible the study of the chemical state of Au by X-ray photoelectron spectroscopy (XPS).

In the last three decades, advanced analytical techniques [such as XPS, X-ray Absorption Fine Structure (XAFS), Mössbauer spectroscopy, and Secondary Ion Mass Spectrometry (SIMS)] have facilitated study of the chemical state of Au in compounds of S. X-ray photoelectron spectroscopy allows one to investigate a wider range of chemical elements than either XAFS or Mössbauer spectroscopy, and probes the chemical state in the surface and near-surface region. The narrow-region XPS signal originates very largely from only the upper  $\sim 15 \text{ \AA}$  of a sample surface (Briggs & Seah 1985) and, hence, may not be representative of the bulk sample. In the earth sciences, the surface-sensitivity of XPS has been used recently to show that  $\text{Au}^+$  can be detected on pyrite surfaces reacted in Au-bearing NaHS solutions (Scaini *et al.* 1998). The  $\text{Au}^+$  species was considered to be an adsorbed Au–SH complex, but the  $\text{Au}^+$  state underwent rapid reduction in sunlight or air exposure. These results differ from the findings of similar studies using chloride solutions. These indicated that aqueous  $\text{Au}^{3+}$  was rapidly adsorbed and reduced directly to  $\text{Au}^0$  on metal–sulfide substrates (Jean & Bancroft 1985, Hyland & Bancroft 1989). XPS analysis of solid Au–S-bearing complexes has been limited to the study of organometallic compounds. Although gold sulfides ( $\text{Au}_2\text{S}$ ,  $\text{Au}_2\text{S}_3$ ) are considered stable at room temperature and pressure (Puddephatt 1978), XPS analysis of these compounds reveals no evidence of  $\text{Au}^+$  (Mycroft *et al.* 1995). This result was attributed to decomposition prior to analysis, or to beam damage during analysis. Several researchers have investigated the interaction of adsorbed  $\text{H}_2\text{S}$  on surfaces of metallic Au (Leavitt & Beebe 1994, Jaffey & Madix 1991), in connection with its catalytic properties and potential use as a substrate for S-containing organic molecules. These studies show that the interaction of thiol groups with Au metal appears to vary with crystallographic orientation; Au–SH groups are stable up to 520 K on (111) surfaces of Au.

XPS has been used also to study the chemical state of Au within “cluster” or polynuclear compounds, which are defined as discrete units containing at least three metal atoms in which metal–metal bonding is present (Johnson 1980). These compounds typically comprise a loose, ordered array of organic ligands around Au–Au metal bridges. Their XPS spectra commonly indicate a binding energy intermediate between that of  $\text{Au}^0$  and  $\text{Au}^+$ , which has led to extensive debate on whether the Au atoms are present in both  $\text{Au}^0$  and  $\text{Au}^+$  chemical states (van Attekum *et al.* 1980) or in an intermediate oxidation state (Battistoni *et al.* 1982, Hall & Mingos 1984).

Other techniques have been applied to the study of the chemical state of Au in association with S and S-bearing compounds. For instance, a substantial fraction of the “invisible” Au content of sulfide and arsenide minerals and experimental products is indicated by electron-probe micro-analysis (EPMA), SIMS, and Mössbauer spectroscopy to be incorporated in a chemically bound state (*e.g.*, Marion *et al.* 1986, Cathelineau *et al.* 1989, Cabri *et al.* 1989, Fleet *et al.* 1993, Mumin *et al.* 1994, Fleet & Mumin 1996). Mössbauer spectroscopy also demonstrates that Au is sorbed as  $\text{Au}^+$  by colloidal  $\text{As}_2\text{S}_3$  and  $\text{Sb}_2\text{S}_3$ , that has reacted with aqueous thio-gold solutions, consistent with the presence of a  $\text{Au}^+$ –HS surface complex (Cardile *et al.* 1993). Recent Hartree–Fock MO (molecular orbital) calculations by Tossell (1996) point to the involvement of  $\text{H}_2\text{O}$  and OH groups in the speciation of Au in aqueous fluids, the predominant species being predicted to be  $\text{Au}(\text{SH})(\text{H}_2\text{O})$  at low pH,  $\text{Au}(\text{SH})^{-1}$  in near-neutral solutions, and  $\text{Au}(\text{SH})(\text{OH})^{-1}$  at high pH.

Despite the apparently common and important association between Au and S, and the increasing number of studies of this relationship, no definitive XPS data have been obtained for the binding energies of  $\text{Au}^+$ –S compounds. In this paper, we present XPS data on the diverse chemical states of Au deposited from fluids in the Mg–S–H–O system, and speculate on the oxidation state of Au in brucite(periclase)-saturated  $\text{H}_2\text{S}$ -rich fluids.

#### EXPERIMENTAL AND ANALYTICAL METHODS

Hydrothermal experiments were performed in Tuttle-type cold-seal bombs, using sealed gold capsules of 2.4 mm ID and 25–38 mm length to contain the reaction, and the capsule metal,  $\text{MgS}$ , and water as reagents. The capsules typically contained 0.02 g  $\text{MgS}$  and 0.03 mL  $\text{H}_2\text{O}$ . Pressure was maintained at  $\sim 0.15 \pm 0.01$  GPa, and experimental temperatures varied from 900 to 100°C, with corresponding run times of 1 day to 32 days (details of a selection of experiments are given in Table 1); other experimental details and results obtained by scanning electron microscopy with energy-dispersion analysis (SEM–EDX), EPMA, and Auger electron spectroscopy will be presented elsewhere. At the termination of the experiment, the capsules were quenched in air and water and opened either in laboratory air or in a  $\text{N}_2$  atmosphere within a glove bag attached to the XPS instrument. Effused fluid products were collected on Al foil, and solid products of the reaction typically were mounted on an adhesive carbon pad. These products were dried either in the vacuum chamber of the XPS or in air.

The X-ray photoelectron spectrometer used for surface analysis was a modified Surface Science Laboratories SSX–100, with a monochromatized  $\text{AlK}\alpha$  X-ray source. The spectrometer work function was

TABLE 1. SEMI-QUANTITATIVE COMPOSITIONS OF SURFACES FROM BROADSCAN XPS ANALYSIS

Expt	T (°C)	P (GPa)	Time (days)	Spot	Products	Mg (at%)	O (at%)	S (at%)	Au (at%)
Solids - air dried									
Mg8	870	0.07	1	1	large, orange-red grains	51.3	32.7	6.7	8.9
				2		41.2	34.7	8.4	15.7
				3		51.2	39.9	5.5	3.4
				4		51.1	37.0	6.9	4.7
Mg21	860	0.14	1	1	single large, deep red grain	41.8	48.3	8.6	1.3
				2	40.9	50.2	7.6	1.3	
				3	38.7	40.0	20.9	0.4	
Mg29	700	0.14	3	1	medium, red grains	33.9	29.7	17.4	19.0
				2	36.7	31.4	22.9	9.0	
Mg37	700-165	0.16	5	1	medium, orange-red grains	35.9	40.3	9.3	14.5
				2	37.7	43.1	8.2	11.0	
Mg39	200	0.14	10	1	single, bright red grain	38.8	45.9	9.1	6.2
Mg41	300	0.13	10	1	small, pale orange grains	33.4	60.6	2.8	3.2
				2	28.7	59.0	11.3	1.0	
				3	24.9	67.0	4.5	3.6	
Solids - vacuum dried									
Mg52	500-295	0.15	2	1		37.8	58.5	3.1	0.6
Mg54	295	0.15	10	1	yellow	50.3	43.2	5.3	1.2
Mg57	595	0.18	4	1	yellow	43.9	52.6	2.7	0.8
Fluids - air dried									
Mg12	860	0.13	1	1	pale orange-red evaporate	40.6	51.7	2.9	4.8
Mg13	865	0.15	1	1	orange-brown evaporate	28.9	50.4	20.1	0.6
Mg14	865	0.15	1	1	orange with yellow patches	41.7	51.8	4.4	2.1
Mg53	295	0.15	12	1	on Al foil	36.4	49.8	11.5	2.3
					on filter paper	39.3	58.7	0.0	2.0
Mg58	700	0.16	2	2	orange-yellow	40.4	51.9	7.0	0.7
Fluids - vacuum dried									
Mg53	295	0.15	10	1	greyish, drying to yellow	36.3	48.6	6.1	9.0
				1	39.8	40.2	15.0	5.0	
Mg54	295	0.15	10	1	grey, drying to yellow	52.4	41.9	3.7	2.0
Mg56	305	0.17	12	1	colourless to yellow	51.4	44.8	3.8	0.0
Mg57	595	0.18	4	1	grey, drying to yellow	47.8	49.2	1.8	1.2
				2	51.3	44.2	2.7	1.8	
Mg58	700	0.16	2	1	yellow	38.9	46.5	12.7	1.9
					38.1	48.3	10.0	3.6	

adjusted to give a value of  $84.00 \pm 0.05$  eV [with peak full-width half-maximum (FWHM) of  $0.8 \pm 0.05$  eV] for the Au  $4f_{7/2}$  peak of metallic Au (Mansour 1996). The energy dispersion was set to give an energy difference of  $857.5 \pm 0.1$  eV between the Cu  $2p_{3/2}$  and Cu  $3p$  lines of metallic Cu. Internal referencing of spectra was made to the C  $1s$  peak of graphite-like C at 285.0 eV to compensate for charging effects in the samples. Survey scans were recorded using a 600  $\mu\text{m}$  spot size and a fixed pass energy of 160 eV, whereas narrow-scan spectra were recorded using a 300  $\mu\text{m}$  X-ray spot and a fixed pass energy of 50 eV. Integrated photoelectron intensities were corrected for the Scofield cross-sections and the inelastic mean free path for kinetic energy. Spin-orbit splitting results in the formation of doublet peaks for S and Au species (Briggs & Seah 1985). The doublet components for

S  $2p_{3/2}$  and S  $2p_{1/2}$  are separated by 1.18 eV with a peak-area ratio of 2:1, and the doublet components for Au  $4f_{7/2}$  and Au  $4f_{5/2}$  are separated by 3.7 eV with a peak-area ratio of  $\approx 1.3:1$  (Moulder *et al.* 1992). Reference binding energies for Au  $4f$  and S  $2p$  species are given in Tables 2 and 3, respectively.

Charge accumulation during XPS analysis was frequently troublesome, resulting in shifts in peak position and peak asymmetry. Various techniques were employed to limit or prevent it, *e.g.*, use of conductive substrates for the samples, an electron floodgun, and a conductive grid placed above the sample. The optimum signal-to-noise and peak shape and form were obtained by applying floodgun electrons of  $\sim 2$  eV. We emphasize that peak shifts due to charging were corrected using the C  $1s$  spectrum, which was collected routinely in this study.

TABLE 2. REFERENCE XPS BINDING ENERGIES FOR Au 4f<sub>7/2</sub> IN INORGANIC AND ORGANOMETALLIC GOLD COMPLEXES

Complex	Binding Energy		Reference
	$\Delta$ Au 4f <sub>7/2</sub> <sup>a</sup> (eV)	Au 4f <sub>7/2</sub> (eV)	
Au <sup>0</sup>	0.0	83.98 (84.0)	Moulder <i>et al.</i> (1992)
Au <sup>0</sup>	-0.1	83.9	Kishi & Ikeda (1974)
Au + Cl <sub>2</sub>	+1.9	85.9	"
AuCN	+1.4	85.4	"
AuCl	+2.2	86.2	"
NaAuCl <sub>4</sub>	+3.4	87.4	"
AuCN	+1.2	85.2	Jean & Bancroft (1985)
KAu(CD) <sub>4</sub>	+3.2	87.2	"
Au <sub>2</sub> O <sub>3</sub>	+5.5	89.5	Aita & Tran (1991)
Au-hydroxide	+7.3	91.3	"
AuL <sup>b</sup>	+1.7	85.7	Battistoni <i>et al.</i> (1982)
Au <sub>2</sub> I <sub>2</sub> I <sub>2</sub>	+0.8	84.8	"
Au <sub>11</sub> L <sub>2</sub> I <sub>5</sub>	+0.8	84.8	"
AuLI	+1.3	85.3	Van Attekum <i>et al.</i> (1980)
AuLCl	+1.6	85.6	"
AuLSCN	+1.7	85.7	"
Au <sub>11</sub> L <sub>2</sub> (SCN) <sub>3</sub>	+1.4	85.4	"
Na <sub>3</sub> Au(S <sub>2</sub> O <sub>3</sub> ) <sub>2</sub>	+1.1	85.1	Hyland & Bancroft (1989)
S-Au-S	+1.0-1.2	85.0-85.2	Van de Vondel <i>et al.</i> (1977)
Au <sup>+</sup> -S	+1.1	85.1	Scaini <i>et al.</i> (1998)

a - relative to Au<sup>0</sup>; b - L = triphenylphosphine

## RESULTS

### Reaction products

Reaction products routinely present at the experimental conditions were brucite, periclase (above 602–612°C), and fluid. MgS was not evident as a reaction product; it was not observed by visual and X-ray diffraction (XRD) examination of quench products or by surface and near-surface analyses by broadscan XPS, SEM-EDX, and EPMA. Magnesium hydroxide sulfate [2MgSO<sub>4</sub>•Mg(OH)<sub>2</sub>], which is similar in structure and composition to caminite

TABLE 3. REFERENCE XPS BINDING ENERGIES FOR S 2p IN INORGANIC SULFUR COMPOUNDS

Complex	$\Delta$ S <sup>a</sup> (eV)	S 2p <sub>3/2</sub> (eV)	Reference
S <sup>0</sup>	0.0	164.0	Moulder <i>et al.</i> (1992)
S <sup>2+</sup>	-3.1, -2.4	160.9-161.6	Mycroft <i>et al.</i> (1990)
S <sub>2</sub> <sup>2+</sup>	-2.2, -1.2	161.8-162.8	"
S <sub>4</sub> <sup>2+</sup>	-1.2, 0.0	162.8-164.0	Terres <i>et al.</i> (1987) Mycroft <i>et al.</i> (1990)
SO <sub>4</sub> <sup>2-</sup>	+4.2, +7.0	168.2-171.0	Moulder <i>et al.</i> (1992)
Au-HS	-1.8, -1.4	162.2-162.6	Leavitt & Beebe (1994)
Au-H <sub>2</sub> S	-1.2, -0.7	162.8-163.3	"
S <sup>2+</sup> on Au	-2.6, -1.0	161.4-163.0	Buckley <i>et al.</i> (1987)

a - relative to S<sup>0</sup>

(Keefer *et al.* 1981, Janecky & Seyfried 1983, Fleet & Knipe 1997), was identified as trace crystals in experiments at 400° and 700°C. Native S was recognized rarely, on the wall at the top of the gold capsule. Brucite also formed by retrogression of periclase during quenching, and as an evaporate phase. The stability of periclase during quenching varied with grain size and quench rate.

The quenched gold capsules had high internal pressure owing to presence of H<sub>2</sub>S gas. On piercing the capsules, fluid products ± entrained solids were commonly ejected under the release of pressure. The solid products were largely in the form of a plug of soft sediment composed of either brucite or periclase + brucite at the bottom of the gold capsule, coated with precipitated Au-S compounds and quench brucite and periclase.

The color of the solid fraction, and of the fluid fraction also, varied with the ambient atmosphere (laboratory air or nitrogen). For capsules opened in laboratory air, the solid reaction-products were green-grey-white and initially moist. They exhibited progressive development of color with drying, from white, to camel, to deep orange-red. The solids were typically massive, with a porous, white interior that graded to orange near the margin, and had a smooth porcelainous surface-layer. The color of the solids bleached after storage for a few weeks in sealed, transparent glass vials. Fluid evaporates were colorless to canary yellow; color developed progressively during drying to a deep red-brown.

For capsules opened in the nitrogen glove bag, the solids were initially light green-yellow, and aged to dark brown. The evaporates were initially colorless, became yellow during XPS analysis, and aged in air storage to a light brown.

Semiquantitative compositional analysis of the surface layers (to about 15 Å depth) by broadscan XPS (Table 1) and of the deeper near-surface by SEM-EDX consistently indicated Mg:O ratios close to brucite stoichiometry for experiments below 602°C, and a mixture of brucite + periclase for experiments at higher temperature.

Sulfur: Au ratios were variable in both broadscan XPS (Table 1) and SEM-EDX analyses, but were close to 1 for the SEM-EDX analysis of the brown coating of solids opened in nitrogen and for several individual broadscan XPS spots. Gold contents locally were appreciably higher by XPS broadscan analysis than by SEM-EDX, consistent with the accumulation of Au at the surface of red-brown-colored samples. Numerous investigations of proximal red or brown coatings and colorless brucite substrates failed to detect significant Au in the latter. Thus, gold was absent from the brucite and periclase sediment coexisting with the high-temperature fluids. Electron-probe micro-analysis of fluid released under nitrogen and evaporated on Al foil gave S:Au ratios of 2:1 to 3:1.

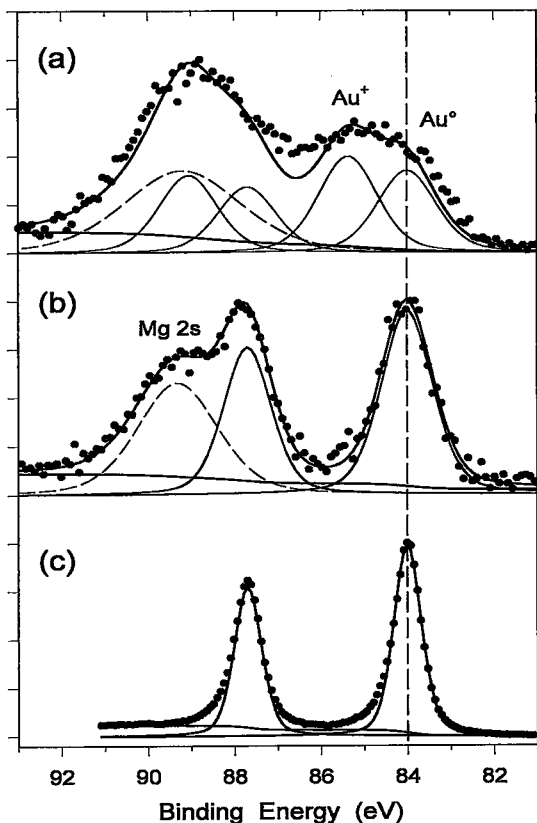


FIG. 1. Narrow-region Au 4f XPS spectra: (a) Gold spectrum from solid reaction-products dried in air (#Mg41; 300°C, 0.13 GPa, 10 d), fitted with peaks for Au<sup>0</sup> at 84.0 eV and Au<sup>+</sup> at 85.3 eV (and doublet peaks) and Mg 2s (89.1 eV; dashed line). (b) Gold spectrum of same solid reaction-products as 1a (*i.e.*, same XPS mount) after exposure to air and light for two weeks. (c) Gold spectrum from pure gold foil, consisting of Au 4f<sub>7/2</sub> peak for Au<sup>0</sup> at 84.0 eV and doublet peak at +3.7 eV. The spectrum of 1b is fitted with peaks for Au<sup>0</sup> and Mg 2s only, and demonstrates complete photo-reduction of all Au<sup>+</sup>. Reference line is position of Au 4f<sub>7/2</sub> peak for Au<sup>0</sup> at 84.0 eV.

#### X-ray photoelectron spectroscopy (XPS) analysis

Narrow-region XPS spectra were acquired for Au 4f, S 2p, C 1s and O 1s spectral regions, but only results for Au (Figs. 1, 2) and S (Fig. 3) are considered here. Carbon spectra were used only for internal referencing, to the C 1s peak of graphite-like C at 285.0 eV. Oxygen data gave little useful information on speciation on the sample surfaces, with the principal O 1s peak being found at ~531 eV, consistent with the presence of hydroxyl species (Thiel & Madey 1987) in brucite. Magnesium was an interference in the study of Au

speciation, because of overlap of the Mg 2s peak at ~89 eV with the Au<sup>0</sup> 4f<sub>5/2</sub> or Au<sup>3+</sup> 4f<sub>7/2</sub> lines.

For solid reaction-products dried in air, the Au XPS spectra were fitted with peaks for Au<sup>0</sup> at 84.0 eV (±0.1 eV) and a second species at 85.3 eV (±0.2 eV) with a full-width at half-maximum (FWHM) of 1.3–1.5 eV (Fig. 1a). The binding energy of the latter species is consistent with Au<sup>+</sup> (Table 2); this species formed up to 60% of the total Au signal. Other solid products yielded spectra with no evidence of Au<sup>+</sup>, although there was no

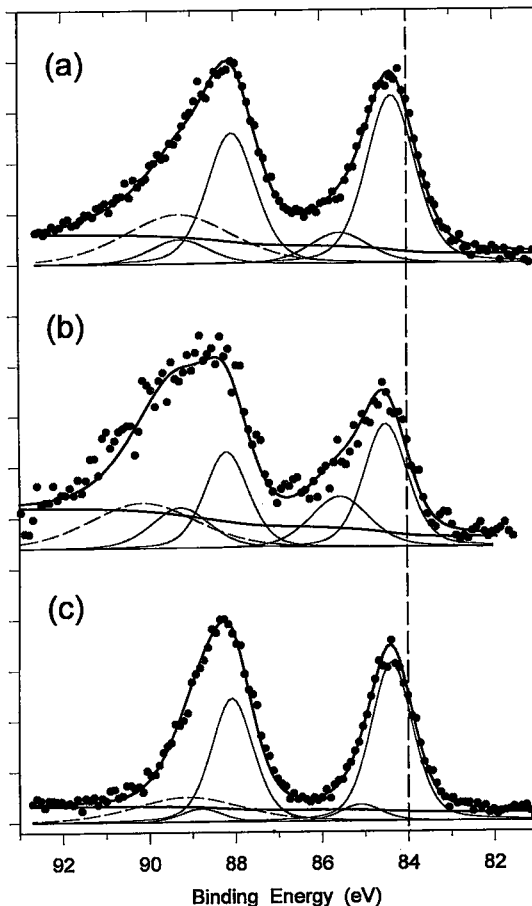


FIG. 2. Narrow-region Au 4f XPS spectra: (a) Fluid reaction-products dried in air (#Mg12; 860°C, 0.13 GPa, 1 d). (b) Solid products dried in vacuum (#Mg54; 295°C, 0.15 GPa, 10 d). (c) Fluid products dried in vacuum (#Mg54). All spectra indicate a dominant contribution from Au, with an apparent state of oxidation intermediate between Au<sup>0</sup> and Au<sup>+</sup>, and consistent with either small (nanoscale) clusters of Au atoms or mononuclear Au<sup>0</sup> complexes. Minor Au<sup>+</sup> is present in solid products dried in vacuum (2b), fluid products dried in air (2a), and, perhaps, also in fluid products dried in vacuum (2c) (*cf.* Fig. 1a). Reference line is position of Au 4f<sub>7/2</sub> peak for Au<sup>0</sup> at 84.0 eV.

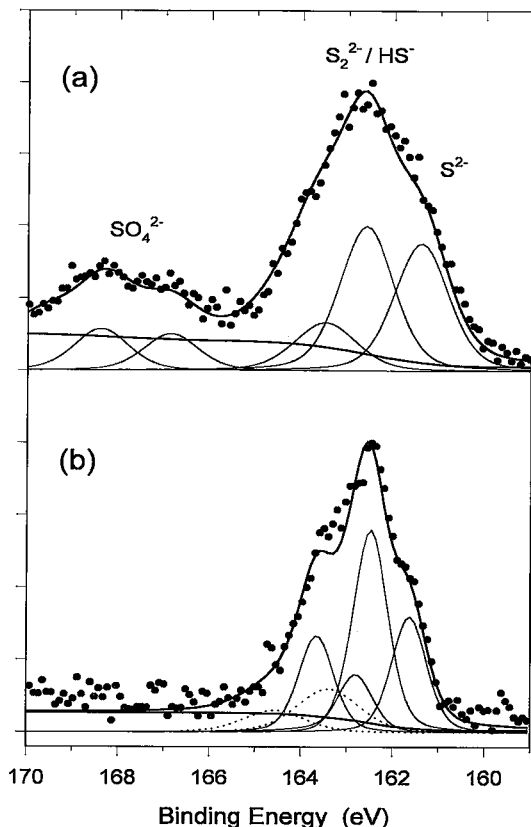


FIG. 3. Narrow-region  $S\ 2p$  XPS spectra: (a) Air-dried orange-red solids (#Mg41; 300°C, 0.13 GPa, 10 d); spectrum reveals monosulfide (signal at 161.4 eV), disulfide/hydrosulfide (162.7 eV), perhaps polysulfide (163.5 eV), and two S–O species (166.8 and 168.3 eV), which are interpreted as thiosulfate and sulfate, respectively (cf. Fleet *et al.* 1993); doublets for S peaks, at +1.18 eV for all species, have been omitted for visual clarity. (b) Air-dried solids attached to gold capsule wall (#Mg38; 200°C, 0.14 GPa, 10 d); spectrum reveals monosulfide (signal at 161.6 eV), disulfide/hydrosulfide (162.5 eV), and perhaps polysulfide (163.4 eV).

obvious correlation between the presence or absence of  $Au^+$  and the experimental conditions. Solid products that had initially produced Au spectra indicating both  $Au^0$  and  $Au^+$  were re-analyzed after exposure to laboratory atmosphere and sunlight for 2–10 weeks. In all cases, these re-acquired Au spectra show a peak for  $Au^0$  only (cf. Figs. 1b, c). The S spectra typically contain a main, broad peak with a centroid at ~162.5 eV, which was fitted with a component for disulfide S ( $S\ 2p_{3/2}$  at 162.4–162.7 eV, FWHM of 1.3 eV), plus a minor monosulfide component ( $S\ 2p_{3/2}$  at 161.4–161.7 eV) (Fig. 3). The S spectra less frequently show weaker peaks at binding energies between 166.8

and 168.3 eV, corresponding to S–O species. These weaker peaks typically comprise less than 20% of the total S signal. The spectrum in Figure 3a indicates the presence of more than one S–O species.

For fluid reaction-products dried in air, all Au spectra were dominated by a single broad peak at ~84.3 eV (with FWHM  $\approx$  1.6 eV) (Fig. 2a). There was also a minor component at ~85.6 eV, which was assigned to  $Au^+$ . The S spectra of the fluid products evaporated on Al foil indicated higher sulfate:disulfide ratios than those of corresponding solid products.

For solid reaction-products dried in vacuum, few spectra were recorded owing to difficulties in retrieving and mounting solid reaction-products for XPS analysis within the inert atmosphere environment. However, all Au spectra that were obtained were fitted with a dominant Au species with a peak centroid about 84.5 eV, and a subordinate Au species with a peak centroid at ~85.6 eV, which was assigned to  $Au^+$  (Fig. 2b). The S spectra were weak, but comprised a single broad peak with a centroid at ~162 eV.

For fluid reaction-products dried in vacuum, all Au spectra essentially comprised a single symmetrical broad peak at ~84.3 eV (with FWHM  $\approx$  1.3 eV; Fig. 2c). The S spectra were again weak and comprised of a single broad peak with a centroid at ~162 eV.

Surface contamination by graphite-like C is unavoidable and ubiquitous in narrow-region XPS spectroscopy. The chemical state of this C is constant from one measurement to another, and its C 1s peak is well resolved from that of C in carbonate or adsorbed  $CO_2$ . Hence, it is common practise to use the C 1s peak for graphite-like C at 285.0 eV to correct for energy shifts due to sample charging in narrow-region XPS spectra (e.g., Fleet *et al.* 1993). Sporadic charging of the samples did not introduce error in the peak positions for Au species. The peaks at 84.5 and 84.3 eV, respectively, that characterize the reduced Au species in solids from capsules opened in an inert atmosphere (Fig. 2b) and in both air- and vacuum-dried fluids (Figs. 2a, c) are well resolved from that for native Au (at 84.0 eV; Fig. 1c) in the present narrow-region Au 4f XPS spectra. We are confident that these higher-energy peaks represent Au in a different chemical state than native Au. The peak assigned to Mg 2s at ~89 eV in Figures 1 and 2 is very broad, and its energy position is variable. It is evident that the precise chemical state of Mg in the present Au-bearing solids and evaporated fluids was too uncertain to use a Mg peak to confirm the correction for charging during the collection of the XPS spectra. We did not attempt to obtain characteristic narrow-region XPS spectra for Mg and S in MgS reagent, to test for the possible presence of MgS in the quench products. Magnesium sulfide is very hygroscopic, and the resulting Mg and S XPS spectra undoubtedly would not have been representative of a pristine anhydrous MgS surface. Also, MgS was not evident as a reaction product in the experiments of

Fleet & Knipe (in progress); *i.e.*, MgS was not detected in broad-scan XPS, SEM-EDX, EPMA, and powder X-ray diffraction studies.

The changes in color noted above in samples removed from the XPS chamber were not attributable to photo-reduction of Au complexes by  $\text{AlK}\alpha$  X-rays. Changes in color of samples from capsules opened in the nitrogen glove bag were not restricted to the local areas investigated by XPS analysis, but rather they were uniform over sample surfaces. We have assumed that the color of evaporated samples and coatings on equilibrium solids is attributable to Au complexes. This assumption is consistent with the broad-scan XPS, SEM-EDX, and EPMA results, which show that Au is restricted to evaporated samples and colored coatings on solids. We further assume that changes in color reflect progressive aging of the Au complexes, which is effected by loss of volatile ligand components and reduction of Au.

## DISCUSSION

### *Quench products*

The experiments of Fleet & Knipe (in progress) resulted in Au solubilities of up to 50,000 mg/kg (at 200°C). During quenching of the experimental charges, an  $\text{H}_2\text{S}$ -rich gas phase separated (*e.g.*, Shvedenkov *et al.* 1986), Au-S compounds precipitated in response to decrease in  $\text{H}_2\text{S}_{(\text{aq})}$  and temperature, periclase (experiments above 602–612°C) partially altered to brucite, and the activity of  $\text{Mg}^{2+}$  in solution increased owing to the retrograde solubility of brucite. The observations of Fleet & Knipe (in progress) and presented here on the solids and evaporates clearly show that all of the solubilized gold was held in solution at the experimental temperature. In particular, higher contents of Au revealed by the surface-sensitive XPS broad-scan technique, compared with the deeper-probing SEM-EDX, and depth profiling by Auger electron spectroscopy all demonstrate that Au was more abundant in the outermost layers of the coatings.

Most of the Au precipitated during the temperature quench and was deposited as an outer coating of Au-S compounds on the equilibrium solids and gold capsule wall. A small fraction of the dissolved Au remained in the temperature-quenched fluid and precipitated when the capsule was pierced and the solids and fluids dried. The chemical state of Au in deposits from this latter fraction is investigated with the fluid products present, whereas Au in the solid products was deposited largely during the temperature quench.

Use of complementary techniques, such as SEM-EDX, broad-scan XPS, and Auger electron spectroscopy, indicates that Au is associated only within the colored reaction and quench products, but is absent from the solid brucite-periclase plug. Gold contents do not correlate with S in the broad-scan XPS

analyses (Table 1), and neither S nor Au correlate strongly with the intensity of coloration of the reaction products. However, the latter can be attributed to the surface sensitivity of XPS analysis. The broad-scan XPS signal is obtained from the surface and near-surface region, whereas the colored surface deposit was evidently tens to hundreds of micrometers in thickness. Gold contents were greatest in the surface and near-surface region, and decreased through the colored surface deposit. The observed change in color with exposure to air and light suggests that the red coloration could be associated with either a change in ligand configuration of Au or S species or formation of colloidal Au. When the experimental capsules were opened, the abrupt loss of  $\text{H}_2\text{S}$  may have resulted in exchange of HS bonded to  $\text{Au}^+$  by OH or  $\text{H}_2\text{O}$ , with stereochemical details varying from sample to sample. Colloidal Au is generally red and may be deep red-brown (J.F. Corrigan, pers. commun. 1997). It is an anticipated product of the reduction of aqueous  $\text{Au}^+$  complexes and, indeed, the XPS spectra of the aged solids present, which are characterized by a broad Au  $4f_{7/2}$  peak at 84.0 eV (Fig. 1b), are most consistent with the dominant presence of colloidal Au. Therefore, the red coloration is most likely attributable to colloidal Au that formed on aging of the Au hydrosulfide deposits. In summary, the colored surface-products *do* appear to indicate that soluble Au precipitated during quenching, but the intensity of color does not necessarily reflect the amount of Au present.

### *XPS peak assignments*

Narrow-region Au  $4f$  XPS spectra from all quenched products, whether acquired on solids or fluids, and whether dried in air or vacuum, showed a principal Au  $4f_{7/2}$  peak shifted positive in binding energy relative to  $\text{Au}^0$  (at 84.0 eV in gold foil). Gold  $4f_{7/2}$  peaks have been fitted at three characteristic binding energies beyond 84.0 eV (Figs. 1, 2): 85.3 eV (solids dried in air), 84.5 eV (solids dried in vacuum), and 84.3 eV (fluids dried in air and vacuum).

Positive chemical shifts of the Au  $4f_{7/2}$  peak beyond 84.0 eV have been attributed variously to:

- 1) *Small size of the particles.* Binding energy shifts for  $\text{Au}^0$   $4f_{7/2}$  of up to +1.2 eV have been recorded for clusters of Au below 100 atoms in size (Dicenzo *et al.* 1988). The shift in binding energy is due to delocalization of electronic charge within the atomic cluster, and is a well-established phenomenon of small metal-atom clusters (Wertheim *et al.* 1986). Using the calibration of Dicenzo *et al.* (1988), a shift of  $\sim+0.4$  eV corresponds to a cluster of  $\sim 33$  Au atoms, and shifts of  $\sim+0.7$ – $1.0$  eV correspond to clusters of  $\sim 5$ – $7$  atoms. However, nanoscale Au particles tend to result in pronounced asymmetry of peaks in Au  $4f$  XPS spectra due to a broad dispersion of cluster size; for example, Mycroft *et al.* (1995) attributed a broad high-energy

shoulder on the Au<sup>0</sup> 4f<sub>7/2</sub> peak to clusters of Au<sup>0</sup> atoms.

2) *Gold cluster compounds.* Cluster compounds typically have a loose ordered structure containing Au atoms within a matrix of organic ligands (commonly triphenylphosphines and triarylphosphines; Hall & Mingos 1984). Gold is considered to reside within the cluster in mixed Au<sup>0</sup> and Au<sup>+</sup> chemical states, but loss of charge is distributed throughout the cluster. Thus, XPS analyses of cluster compounds tend to yield Au 4f<sub>7/2</sub> spectra comprising a single broad peak, with a binding energy intermediate between those of Au<sup>0</sup> and chemically bonded Au<sup>+</sup> (Battistoni *et al.* 1982).

3) *Chemisorbed Au complexes and weakly chemically bonded Au.* Gold may be weakly bonded chemically to ligand species. In the present context, the ligand would be hydrosulfide (HS<sup>-</sup>), which is known to readily bond with Au (*e.g.*, Leavitt & Beebe 1994, Jaffey & Madix 1991).

4) *Chemically bonded Au complexes.* Stable Au<sup>+</sup> and Au<sup>3+</sup> compounds exhibit a significant positive chemical shift in binding energy relative to Au<sup>0</sup>. Au<sup>+</sup> complexes have binding energies of 85.1–86.2 eV, whereas Au<sup>3+</sup> complexes have binding energies of 87.2–91.3 eV (Table 2), which are significantly higher than those recorded in the present study.

In practise, Au 4f<sub>7/2</sub> peak assignments are based on both the magnitude of the peak shift (relative to Au<sup>0</sup>) and peak shape. The experimental system, method of sample formation, and sample morphology may also have a bearing on peak assignments.

Narrow-region XPS scans of the present solid products dried in air commonly showed evidence for two Au species, with Au 4f<sub>7/2</sub> peaks at 84.0 eV and 85.3±0.2 eV (and doublet peaks at +3.7 eV). The species at 84.0 eV corresponds to Au<sup>0</sup>, and the species at 85.3 eV is attributed to Au<sup>+</sup>, and assigned to an Au–S complex. The Au<sup>+</sup> hydroxide and Au<sub>2</sub>O compounds cannot have formed (Puddephatt 1978), although mixed Au–HS–H<sub>2</sub>O or OH complexes may be important in some aqueous solutions (Tossell 1996). A value of the binding energy of 85.1 eV has been attributed to Au<sup>+</sup> adsorbed on pyrite substrates, through a proposed S–Au–S bond (Scaini *et al.* 1998), where one S atom is part of the substrate and the other is bonded to an adsorbed hydrosulfide group. This binding energy corresponds well to that measured for S–Au–S bonding within organometallic compounds (85.0–85.2 eV; Van de Vondel *et al.* 1977). The binding energy recorded in this study (85.3 eV) is marginally elevated compared to that in these documented Au–S species, and thus possibly represents a Au<sup>+</sup> thiosulfate [*e.g.*, Au(S<sub>2</sub>O<sub>3</sub>)<sub>2</sub><sup>3-</sup>], perhaps formed as an oxidation product of an Au–S complex, prior to reduction to Au<sup>0</sup>. XPS binding energies are proportional to the covalency and strength of bonding with the complexing ligand. A general trend exists, with AuCN (which has a high bond-strength; Seward 1991) having a binding energy of 85.2 eV, and AuCl (less strongly bonded) having a binding energy

of 86.2 eV. Gold-thio complexes [*e.g.*, AuHS<sup>0</sup> and Au(S<sub>2</sub>O<sub>3</sub>)<sub>2</sub><sup>3-</sup>] lie between the chloride and cyanide complexes in bond strength (Seward 1991) and, therefore, should have intermediate binding energies. Loss of the Au<sup>+</sup> signal after exposure to air and daylight for several weeks (Fig. 1b) is consistent with the known photo-reducibility of Au–S compounds (T.M. Seward, pers. commun. 1995).

A Au 4f<sub>7/2</sub> peak position of 85.3±0.2 eV is fully consistent with the Au<sup>+</sup> state. We appreciate that there is minor overlap with the upper-bound value of peak position for very small clusters of Au atoms, but note that a Au cluster assignment for the 85.3 eV peak is excluded by the asymmetry of the overall peak envelope. Gold clusters typically result in a high-energy shoulder to the Au 4f<sub>7/2</sub> peak. The spectrum in Figure 1a reveals a low-energy shoulder to the Au 4f<sub>7/2</sub> peak envelope, and this is appropriately interpreted as a Au<sup>0</sup> 4f<sub>7/2</sub> peak superimposed on a Au<sup>+</sup> 4f<sub>7/2</sub> peak.

The Au 4f XPS spectra of vacuum-dried solids indicate the possible presence of two Au species, based on Au 4f<sub>7/2</sub> peaks fitted with binding-energy centroids of ~84.5 eV and ~85.5 eV (Fig. 2). The latter of these peaks is subordinate, forming a high-energy shoulder to the main peak, but the binding energy conforms with that of the Au<sup>+</sup> thio complex considered above. The position of the main Au 4f<sub>7/2</sub> peak is shifted considerably away from that of Au<sup>0</sup>. The binding energy is too low for any known Au<sup>+</sup> complex (Table 2), but is at the upper end of binding energies for small clusters of Au atoms.

The Au 4f XPS spectra for both air and vacuum-dried fluid products indicate the presence of a dominant Au species, with a main peak centroid at about 84.3 eV. This peak is broad and shifted by approximately +0.3 eV from that of Au<sup>0</sup>. Therefore, this simple XPS spectrum could represent small clusters of Au<sup>0</sup> atoms, with a mean cluster size of ~35–50 Å. Alternatively, the shift in binding energy is within the range predicted for Au attached to SH (after Leavitt & Beebe 1994). Thus, mononuclear Au<sup>0</sup> complexes are quite likely.

The present S 2p XPS spectra for air-dried samples are complex, and can be fitted with contributions from up to five species (Fig. 3). Commonly, there is signal from monosulfide, hydrosulfide or disulfide ± polysulfide species (at 161.4–163.8 eV), and one or more S–O species (at 167.0–168.5 eV). Present assignments are based on typical reference binding energies for compounds of S (Table 3); reference XPS data for S species in the Mg–S–O–H system are not available. The position of the most intense peak (162.4–162.7 eV) conforms to the binding energy cited for HS attached to Au metal (Leavitt & Beebe 1994). The minor S 2p signal at ~163.5 eV lies at a binding energy normally attributed to polysulfide species (*cf.* Table 3), although this value also is close to the binding energy cited for H<sub>2</sub>S attached to Au (163.2–162.7 eV; Leavitt & Beebe 1994). Unfortunately, there is no accompanying binding

energy for Au attached to HS. A disulfide species is also consistent with the position of the main peak (Table 3). A sulfate component is common to all of the acquired S spectra, although it is characteristically less intense than the main peak at ~162.4–162.7 eV. The increase in proportion of the sulfate signal after solids were exposed to the atmosphere for a number of weeks is consistent with the formation of  $\text{MgSO}_4 \cdot x\text{H}_2\text{O}$  from oxidation in air. The rare presence of a second S–O species (~167.0 eV; cf. Fig. 3a) is intriguing, since this may represent a thiosulfate complex, either of Mg or Au. The S 2*p* XPS spectra for samples prepared in an inert atmosphere and vacuum dried were also dominated by a peak attributable to either hydrosulfide or disulfide species. Features attributable to oxidized S species were present only in spectra re-acquired after samples were exposed to air.

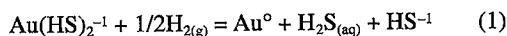
### Chemistry of deposited gold

The present observations suggest that  $\text{Au}^+$ –S complexes and the  $\text{Au}^+$  oxidation state are dominant in the experimental system only at high fugacity of  $\text{H}_2\text{S}$ . Because of the very high contents of solubilized Au (both in solution and precipitated during the temperature quench), the rapid release of  $\text{H}_2\text{S}$  stripped the stabilizing hydrosulfide groups from the  $\text{Au}^+$ –S complexes and promoted reduction of the Au. For fluid and solids sampled in the inert ( $\text{N}_2$ ) atmosphere, the change in the chemical state of Au in the surface and near-surface was essentially homogeneous. Precipitation of native Au did not occur, but this can be attributed to the low temperature at which the capsules were pierced (*i.e.*, insufficient activation energy to nucleate and grow crystals). Interestingly, 5–30  $\mu\text{m}$  crystals of native Au were found in the few experiments that failed during the temperature quench. Also, the soluble Au–S complexes may have precipitated metastably (*e.g.*, by an abrupt change in pH) or  $\text{Au}^+$ –SH bonds may have been sufficiently strong to retard collapse of the complexes until after precipitation. Within the brucite–periclase sediment, mobility of the Au atoms would have been limited to the growth of just nanoscale clusters. We note that atomic clusters of Au, ranging from colloidal size down to just a few atoms stabilized by an outer shell of ligands, form readily by mixing fairly simple inorganic solutions (*e.g.*, Kreibig & Vollmer 1995). Alternatively, the reduced Au may have been present as mononuclear  $\text{Au}^0$  complexes. For solid samples exposed to air, photoreduction of Au was accompanied by partial oxidation of S to thiosulfate which, in complexing with  $\text{Au}^+$ , may have been responsible for partial preservation of the  $\text{Au}^+$  species.

The generally low S:Au ratios in Au-bearing surfaces (Table 1) and the need for a reducing agent for  $\text{Au}^+$  are important constraints on speciation of deposited Au and the present hypothetical reconstruc-

tions for Au precipitation. The large variation in S:Au ratio determined by XPS broad-scan analysis (Table 1), both among and within samples, shows that total S is not strongly coupled with Au. Therefore, for present purposes, minimum values of the S:Au ratio are more significant than maximum values. Gold–hydrosulfide complexes are thought to involve few Au–S bonds (1 or 2; *e.g.*, Benning & Seward 1996). Also, more generally, in inorganic compounds  $\text{Au}^+$  prefers linear complexes with simple ligands (two-fold coordination) or complexes that are intermediate between two- and three-coordinate (*e.g.*, Cotton & Wilkinson 1988), although this stereochemical preference does not necessarily constrain the total-S:Au ratio. For reduced Au deposited by evaporation of the present fluids, a low S:Au ratio seems more consistent with the presence of clusters of Au atoms than with mononuclear  $\text{Au}^0$  complexes; *e.g.*, in experiment Mg12 (Table 1, Fig. 2a), S apparently is subordinate to Au. Furthermore, for the air-exposed solids, the minimum values suggest S:Au  $\approx$  1 for the deposited Au–S complex (*e.g.*, Mg41; Table 1, Fig. 1a). Thus,  $\text{Au}^+$  thiosulfates [such as the hypothetical compound  $\text{MgHAu}(\text{S}_2\text{O}_3)_2$ ] and  $\text{Au}^+$  disulfides (which both have S:Au  $\geq$  2) appear to be less likely than  $\text{Au}^+$  hydrosulfides (*e.g.*, AuHS).

The confirmed presence of sulfate and possible presence of thiosulfate in the air-exposed solids (*e.g.*, Fig. 3a) points to S as a likely reducing agent for  $\text{Au}^+$  in the fluid samples and solids opened in the inert atmosphere. Monovalent gold is unlikely to have been reduced through Seward's (1973) reaction:



because  $\text{H}_2$  also would have been lost on piercing the capsules. However,  $\text{Au}^+$  could have been reduced by the oxidation of hydrosulfide to polysulfide, and small amounts of polysulfide (particularly of disulfide) would have been obscured by the complexity of the S 2*p* XPS spectrum. Indeed, disulfides do have similar binding energies to hydrosulfides (Table 3); the present assignment of the main peak in the S 2*p* XPS spectra (Fig. 3) to hydrosulfide is based on the dominance of  $\text{H}_2\text{S}$  species [ $\text{H}_2\text{S}(\text{aq})$ ,  $\text{H}_2\text{S}(\text{g})$ ] in the experimental system and the XPS broad-scan results, which indicate low S:Au ratios.

This study has shown that MgS reagent may be used to obtain the high concentrations of  $\text{H}_2\text{S}(\text{aq})$  required for the quantitative precipitation of Au from Au–hydrosulfide-bearing fluids. Unfortunately, there were few literature studies on Au hydrosulfides to guide interpretation of the XPS spectra. Measurements on labeled compounds can be ambiguous, but their synthesis should be attempted in future studies. Also, the possibility of an active role for Mg could be evaluated by using ammonium sulfide or pressurized  $\text{H}_2\text{S}$  starting reagent instead of MgS, as one reviewer has suggested.

*Implications for the geochemistry and mineralogy gold*

We presently confirm the presence of Au<sup>+</sup> and reduced Au in precipitates formed during the temperature quench of Mg–S–H–O fluids. Precipitation of Au<sup>+</sup> hydrosulfide is independent confirmation of the Mössbauer spectroscopy study of Cardile *et al.* (1993), who showed that Au was removed from aqueous NaHS solutions as Au<sup>+</sup> sorbed by colloidal As<sub>2</sub>S<sub>3</sub> and Sb<sub>2</sub>S<sub>3</sub>. Given the extensive literature on the chemical state of Au in hydrosulfide solutions (*in* Benning & Seward 1996) and analysis of the solubility of Au in the present Mg–S–OH–O fluids (Fleet & Knipe, *in progress*), as well as the greater probability for reduction of Au rather than oxidation during quenching and release of H<sub>2</sub>S gas, the Mössbauer results of Cardile *et al.* (1993) and XPS spectroscopy results of this study provide strong evidence for the predominance of Au<sup>+</sup> in aqueous sulfidic ore fluids.

For samples collected in an inert atmosphere or by evaporation of fluids, we have established that Au in surface layers of the deposits is present as small clusters of Au<sup>0</sup> atoms (or possibly as mononuclear Au<sup>0</sup>). This observation may have bearing on the physical state of invisible Au in ore minerals. Fleet & Mumin (1997) recently suggested that invisible Au in arsenian pyrite and in marcasite and arsenopyrite from sediment-hosted gold deposits represents Au removed from ore fluids by chemisorption at As-rich, Fe-deficient surface sites and incorporated in the solids in metastable solid-solution. However, they recognized that the oxidation state of Au remains uncertain, because the chemisorption process was intrinsically nonsystematic in terms of crystal-chemical parameters and did not yield definitive trends of atomic substitution. Thus, following the present observations, Au could be deposited directly as mononuclear Au<sup>0</sup> in defect surface-sites of these ore minerals during episodic fluctuations in ore-fluid conditions. Incorporation of nanoscale clusters of Au atoms also is feasible. However, there is little direct evidence on the nature of invisible Au favoring colloidal Au to the exclusion of structurally bound Au. Small clusters of Au atoms are not revealed routinely as defects in high-resolution transmission electron microscopy (HRTEM) images of auriferous arsenian pyrite, marcasite and arsenopyrite (*cf.* Bakken *et al.* 1991).

Finally, we have demonstrated deposition of Au by loss of H<sub>2</sub>S and reduction in the absence of metal sulfides (*cf.* Jean & Bancroft 1985, Mycroft *et al.* 1995). Although we recognize the role of pyrite in the deposition of Au by sorption and reduction in gold-depositing systems, the present study clearly shows that direct precipitation as native gold and Au<sup>0</sup> clusters or mononuclear Au<sup>0</sup> (Fig. 2) must occur also, particularly in response to episodic changes in ore-fluid conditions (*e.g.*, rapid drop in temperature, release of pressure, and boiling).

## ACKNOWLEDGEMENTS

We thank three unnamed reviewers for helpful comments, Surface Science Western for assistance with XPS analysis, and the Natural Sciences and Engineering Research Council of Canada for financial support.

## REFERENCES

- AITA, C.R. & TRAN, C.T. (1991): Core level and valence band X-ray photoelectron spectroscopy of gold oxide. *J. Vac. Sci. Technol.* **A9**, 1498–1500.
- BAKKEN, B.M., FLEMING, R.H. & HOCHHELLA, M.F., JR. (1991): High-resolution microscopy of auriferous pyrite from the Post deposit, Carlin district, Nevada. *In* Process Mineralogy XI. Characterization of Metallurgical and Recyclable Products (D.M. Hausen, W. Petruk, R.D. Hagni & A. Vassiliou, eds.). The Minerals, Metals, and Materials Society, Warrendale, Pennsylvania (13–23).
- BATTISTONI, C., MATTOGNO, G., ZANONI, R. & NALDINI, L. (1982): Characterisation of some gold clusters by X-ray photoelectron spectroscopy. *J. Electron Spectroscopy* **28**, 23–31.
- BENNING, L.G. & SEWARD, T.M. (1996): Hydrosulphide complexing of Au<sup>+</sup> in hydrothermal solutions from 150–400°C and 500–1500 bar. *Geochim. Cosmochim. Acta* **60**, 1849–1871.
- BRIGGS, D. & SEAH, M.P. (1985): *Practical Surface Analysis – by Auger and X-ray Photoelectron Spectroscopy*. Wiley, Chichester, U.K.
- BUCKLEY, A.N., HAMILTON, I.C. & WOODS, R. (1987): An investigation of the sulphur(-II)/sulphur(0) system on gold electrodes. *J. Electroanal. Chem.* **216**, 213–227.
- CABRI, L.J., CHRYSOULIS, S.L., DE VILLIERS, J.P.R., LAFLAMME, J.H.G. & BUSECK, P.R. (1989): The nature of “invisible” gold in arsenopyrite. *Can. Mineral.* **27**, 353–362.
- CARDILE, C.M., CASHION, J.D., MCGRATH, A.C., RENDERS, P.A. & SEWARD, T.M. (1993): <sup>197</sup>Au Mössbauer study of Au<sub>2</sub>S and gold adsorbed onto As<sub>2</sub>S<sub>3</sub> and Sb<sub>2</sub>S<sub>3</sub> substrates. *Geochim. Cosmochim. Acta* **57**, 2481–2486.
- CATHELINEAU, M., BOIRON, M.-C., HOLLIGER, P., MARION, P. & DENIS, M. (1989): Gold in arsenopyrites: crystal chemistry, location and state, physical and chemical conditions of deposition. *Econ. Geol., Monogr.* **6**, 328–341.
- COTTON, F.A. & WILKINSON, G. (1988) *Advanced Inorganic Chemistry* (fifth ed.). John Wiley & Sons, New York, N.Y.
- DICENZO, S.B., BERRY, S.D. & HARTFORD, E.H., JR. (1988): Photoelectron spectroscopy of single-size gold clusters collected on a substrate. *Phys. Rev.* **B 38**, 8465–8468.

- FLEET, M.E., CHRYSOULIS, S.L., MACLEAN, P.J., DAVIDSON, R. & WEISENER, C.G. (1993): Arsenian pyrite from gold deposits: Au and As distribution investigated by SIMS and EMP, and colour staining and surface oxidation by XPS and LIMS. *Can. Mineral.* **31**, 1-17.
- \_\_\_\_\_ & KNIPE, S.W. (1997): Structure of magnesium hydroxide sulfate [ $2\text{MgSO}_4 \cdot \text{Mg}(\text{OH})_2$ ] and solid solution in magnesium hydroxide sulfate hydrate and caminitite. *Acta Crystallogr.* **B53**, 358-363.
- \_\_\_\_\_ & MUMIN, A.H. (1997): Gold-bearing arsenian pyrite and marcasite and arsenopyrite from Carlin Trend deposits and laboratory synthesis. *Am. Mineral.* **82**, 182-193.
- HALL, K.P. & MINGOS, D.M.P. (1984): Homo- and heteronuclear cluster compounds of gold. In *Progress in Inorganic Chemistry* **32** (S.J. Lippard, ed.). Wiley, New York, N.Y. (237-325).
- HYLAND, M.M. & BANCROFT, G.M. (1989): An XPS study of gold deposition at low temperatures on sulphide minerals: reducing agents. *Geochim. Cosmochim. Acta* **53**, 367-372.
- JAFFEY, D.M. & MADIX, R.J. (1991): The adsorption of hydrogen sulfide on clean and sulfided Au (110). *Surf. Sci.* **258**, 359-375.
- JANECKY, D.R. & SEYFRIED, W.E., JR. (1983): The solubility of magnesium-hydroxide-sulfate-hydrate in seawater at elevated temperatures and pressures. *Am. J. Sci.* **283**, 831-860.
- JEAN, G.E. & BANCROFT, G.M. (1985): An XPS and SEM study of gold deposition at low temperature on sulphide surfaces: concentration of gold by adsorption/reduction. *Geochim. Cosmochim. Acta* **49**, 979-987.
- JOHNSON, B.F.G. (1980): *Transition Metal Clusters*. John Wiley & Sons, Chichester, U.K.
- KEEFER, K.D., HOHELLA, M.F., JR. & DE JONG, B.H.W.S. (1981): The structure of the magnesium hydroxide sulfate hydrate  $\text{MgSO}_4 \cdot \text{Mg}(\text{OH})_2 \cdot \text{H}_2\text{O}$ . *Acta Crystallogr.* **B37**, 1003-1006.
- KISHI, K. & IKEDA, S. (1974): X-ray photoelectron spectroscopic study of the reaction of evaporated metal films with chlorine gas. *J. Phys. Chem.* **78**, 107-112.
- KREIBIG, U. & VOLLMER, M. (1995): *Optical Properties of Metal Clusters*. Springer-Verlag, Berlin, Germany.
- LEAVITT, A.J. & BEEBE, T.P., JR. (1994): Chemical reactivity studies of hydrogen sulfide on Au (111). *Surf. Sci.* **314**, 23-33.
- MANSOUR, A.N. (1996): Gold Mg K XPS spectra from the Physical Electronics Model 5400 spectrometer. *Surf. Sci. Spectra* **3**(3), 197-201.
- MARION, P., REGNARD, J.-R. & WAGNER, F.E. (1986): Etude de l'état chimique de l'or dans des sulfures aurifères par spectroscopie Mössbauer de  $^{197}\text{Au}$ : premiers résultats. *C.R. Acad. Sci., Paris* **302**, II, 571-574.
- MOULDER, J. F., STICKLE, W.F., SOBOL, P.E. & BOMBEN, K.D. (1992): *Handbook of X-ray Photoelectron Spectroscopy*. Perkin Elmer Corporation, Norwalk, Connecticut.
- MUMIN, A.H., FLEET, M.E. & CHRYSOULIS, S.L. (1994): Gold mineralisation in As-rich mesothermal gold ores of the Bogosu-Prestea mining district of the Ashanti gold belt, Ghana: remobilisation of "invisible" gold. *Mineral. Deposita* **29**, 445-460.
- MYCROFT, J.R., BANCROFT, G.M., MCINTYRE, N.S. & LORIMER, J.W. (1995): Spontaneous deposition of gold on pyrite from solutions containing Au (III) and Au (I) chlorides. I. A surface study. *Geochim. Cosmochim. Acta* **59**, 3351-3365.
- \_\_\_\_\_, \_\_\_\_\_, \_\_\_\_\_, \_\_\_\_\_ & HILL, I.R. (1990): Detection of sulphur and polysulphides on electrochemically oxidised pyrite surfaces by X-ray photoelectron spectroscopy and Raman spectroscopy. *J. Electroanal. Chem.* **292**, 139-152.
- PUDDEPHATT, R.J. (1978): *The Chemistry of Gold*. Elsevier, Amsterdam, The Netherlands.
- SCAINI, M.J., BANCROFT, G.M. & KNIPE, S.W. (1998): Reactions of aqueous gold(I) sulfide species with pyrite as a function of pH and temperature. *Am. Mineral.* (in press).
- SEWARD, T.M. (1973): Thio complexes of gold and the transport of gold in hydrothermal ore solutions. *Geochim. Cosmochim. Acta* **37**, 379-399.
- \_\_\_\_\_ (1991): The hydrothermal geochemistry of gold. In *Gold Metallogeny and Exploration* (R.P. Foster, ed.). Blackie and Sons, London, U.K.
- SHVEDENKOV, G.YU., KALININ, D.V. & NAZAROV, V.V. (1986): Thermodynamics of liquid-gas equilibrium in the system  $\text{H}_2\text{O}-\text{H}_2\text{S}$ . *Geochim. Int.* **23**(8), 112-123.
- TERMES, S.C., BUCKLEY, A.N. & GILLARD, R.D. (1987):  $2p$  electron binding energies for the sulphur atoms in metal polysulphides. *Inorg. Chim. Acta* **126**, 79-82.
- THIEL, P.A. & MADEY, T.E. (1987): The interaction of water with solid surfaces: fundamental aspects. *Surf. Sci. Rep.* **7**, 211-385.
- TOSSELL, J.A. (1996): The speciation of gold in aqueous solution: a theoretical study. *Geochim. Cosmochim. Acta* **60**, 17-29.
- VAN ATTEKUM, P.M.T.M., VAN DER VELDEN, J.W.A. & TROOSTER, J.M. (1980): X-ray photoelectron spectroscopy study of gold cluster and gold(I) phosphine compounds. *Inorg. Chem.* **19**, 701-704.
- VAN DE VONDEL, D.F., VAN DER KELEN, G.P., SCHMIDBAUR, H., WOLLEBEN, A. & WAGNER, F.E. (1977): ESCA study of organometallics. *Physica Scripta* **16**, 364-366.
- WERTHEIM, G.K., DICENZO, S.B. & BUCHANAN, D.N.E. (1986): Noble- and transition-metal clusters: the d bands of silver and palladium. *Phys. Rev.* **B33**, 5384-5390.

Received April 7, 1997, revised manuscript accepted October 14, 1997.